Investigation of $Zn_{1-x}Cd_xO$ films bandgap and $Zn_{1-x}Cd_xO$/ZnO heterojunctions band offset by x-ray photoelectron spectroscopy*

Jie Chen(陈杰), Xue-Min Wang(王雪敏), Ji-Cheng Zhang(张继成), Hong-Bu Yin(尹泓卜), Jian Yu(俞健), Yan Zhao(赵妍)†, and Wei-Dong Wu(吴卫东)‡

Science and Technology on Plasma Physics Laboratory, Research Center of Laser Fusion, China Academy of Engineering Physics, Mianyang 621900, China

(Received 1 March 2017; revised manuscript received 19 April 2017; published online 20 June 2017)

A series of $Zn_{1-x}Cd_xO$ thin films have been fabricated on sapphire by pulsed-laser deposition (PLD), successfully. To investigate the effect of Cd concentration on structural and optical properties of $Zn_{1-x}Cd_xO$ films, x-ray diffraction (XRD), ultraviolet-visible spectroscopy (UV-vis), and x-ray photoelectron spectroscopy (XPS) are employed to characterize the films in detail. The XRD pattern indicates that the $Zn_{1-x}Cd_xO$ thin films have high single-orientation of the c axis. The energy bandgap values of ZnCdO thin films decrease from 3.26 eV to 2.98 eV with the increasing Cd concentration (x) according to the $(\alpha h\nu)^2$–$h\nu$ curve. Furthermore, the band offsets of $Zn_{1-x}Cd_xO$/ZnO heterojunctions are determinated by XPS, indicating that a type-I alignment takes place at the interface and the value of band offset could be tuned by adjusting the Cd concentration.

Keywords: ZnCdO film, ZnCdO/ZnO heterojunction, optical bandgap, band offset

PACS: 73.61.Ga, 78.20.Ci, 68.60.–p **DOI:** 10.1088/1674-1056/26/8/087309

1. Introduction

Recently, ZnO-based semiconductors have attracted a great deal of attention to light-emitting diodes (LEDs), laser diodes (LDs) operating in the visible and ultraviolet region, owing to its direct wide bandgap (3.37 eV) and large exciton binding energy (60 meV) at room temperature.[1,2] In order to design ZnO-based optoelectronic devices, it is important to realize the adjusting of the bandgap and band offset by doping.[3] Therefore, there have been a number of recent reports on ZnMgO,[4,5] ZnCaO,[6] and ZnSiO,[7] which are wide bandgap semiconductors for wide application in p–n junctions and quantum well-related devices, etc.[8] On the other hand, both theoretical analysis and experimental results illustrate that the bandgap of ZnCdO with different Cd concentration can achieve luminescence from ultraviolet to green light spectra, owing to the smaller bandgap of CdO (2.3 eV).[9,10] Besides, it is very necessary to regulate the bandgap and band offset for adjusting well–barrier height and width. The band diagram of the heterostructure interface is also valuable too. There are several methods to fabricate ZnCdO film, including MBE, PLD, etc.[11–14] PLD is easier to achieve the epitaxial growth of oxide-film than other technology.[15] Kang *et al.*[10] and Sadofev *et al.*[16] fabricated a series of $Zn_{1-x}Cd_xO$ films and had got different bandgaps through adjusting the growth temperature. However, the temperature not only can be used to adjust the Cd concentration, but also affect the film quality.[17] Chen *et al.*[18] fabricated a $Zn_{0.95}Cd_{0.05}O$/ZnO heterojunction, and measured the conduction (valence) band offset by XPS. Theoretically, Tang *et al.*[9] and Luo *et al.*[19] have used first-principles to research the effect of Cd concentration to the $Zn_{1-x}Cd_xO$ bandgap. However, there have been few experimental results reported yet. In this paper, a series of $Zn_{1-x}Cd_xO$ thin films and $Zn_{1-x}Cd_xO$/ZnO heterojunctions were fabricated by using ZnCdO targets which have different Cd concentrations with constant temperature. The structural property and optical bandgap of $Zn_{1-x}Cd_xO$ thin films dependence of Cd concentration were discussed, and then we measured the conduction (valence) band offset of $Zn_{1-x}Cd_xO$/ZnO heterojunctions and analyzed the effect of Cd concentration to the band offset.

2. Experiment

$Zn_{1-x}Cd_xO$ thin films were deposited on sapphire substrate by PLD. Table 1 shows the experimental parameters for the growth of ZnCdO film and ZnCdO/ZnO heterojunction. The KrF excimer laser (248 nm, 2 Hz, 25 ns) with laser power density of 1 J/cm^2–2 J/cm^2 was used as a laser light source. The ZnCdO targets with different Cd concentration were fabricated by mixing ZnO (in purity 99.99%) and CdO (in purity 99.99%) powder. The experiment was carried out in an ultra-high vacuum (1×10^{-7} Pa), and the distance from substrate to target was 5 cm. Firstly, the substrate was heated and degassed 60 min at 600 °C. After that the temperature was lowered to 500 °C. ZnCdO thin films (100 nm) and

*Project supported by the National Natural Science Foundation of China (Grant No. 11404302) and the Laser Fusion Research Center Funds for Young Talents (Grant No. RCFPD1-2017-9).

†Corresponding author. E-mail: zhaoyan267@163.com

‡Corresponding author. E-mail: wuweidongding@163.com

© 2017 Chinese Physical Society and IOP Publishing Ltd

ZnCdO (∼ 5 nm)/ZnO (∼ 100 nm) heterojunctions were deposited on the sapphire substrate. The crystallographic structures of $Zn_{1-x}Cd_xO$ thin films were investigated by XRD. The absorption coefficients of $Zn_{1-x}Cd_xO$ thin films with different Cd concentration were calculated by UV-vis transmittance (T) and reflectance (R), and the optical bandgaps were obtained at the same time. To confirm the Cd concentration in $Zn_xCd_{1-x}O$ thin films and the band offset of $Zn_xCd_{1-x}O$/ZnO heterojunctions, XPS was carried out. The pure ZnO film is named as sample 1, and the samples 2–6 represent the $Zn_xCd_{1-x}O$ films and $Zn_xCd_{1-x}O$/ZnO heterojunctions ($x = 5.0\%$, 6.6%, 7.5%, 8.2%, and 10.0%), respectively. $Zn_xCd_{1-x}O$ films and $Zn_xCd_{1-x}O$/ZnO heterojunctions with the same Cd concentrations have been marked as the same number.

Table 1. The experimental parameters for $Zn_{1-x}Cd_xO$ film and $Zn_{1-x}Cd_xO$/ZnO heterojunction fabrications.

Experiment conditions	Experiment parameters
Working vacuum	1×10^{-7} Pa
Target	ZnCdO and ZnO (purity> 99.99%)
Substrate	Al_2O_3 (0001)
Laser pulse frequency	2 Hz
Laser power density	1 J/cm^2–2 J/cm^2
Deposition time	30 min
The distance between the target and substrate	5 cm

3. Results and discussion

Figure 1(a) shows the XPS survey spectrum of the ZnCdO and ZnO thin films. It can be seen that the Cd peak appears in the ZnCdO film, which indicates that Cd has been dopped in ZnO. The binding energies are accurate on an absolute scale within 0.02 eV–0.04 eV according to test data provided by the XPS manual. Figures 1(b) and 1(c) are the high-resolution scans of Zn 2p and Cd 3d, respectively. The Zn 2p3/2 and Zn 2p1/2 peaks locate at 1024.11±0.02 eV and 1047.13±0.02 eV, Cd 3d5/2 and Cd 3d3/2 peaks locate at 407.50±0.02 eV and 414.27±0.02 eV, respectively. The molar ratio of Cd and Zn in $Zn_{1-x}Cd_xO$ is calculated by using the standard formula $n_a/n_b = \beta_b I_a/\beta_a I_b$ (I: XPS peak intensity; β: sensitivity factor), the results are shown in Table 2. It is worth noting that the Cd concentration in $Zn_{1-x}Cd_xO$ films (5.0%, 6.6%, 7.5%, 8.2%, and 10.0%) is much smaller than that in the targets, which could be ascribed to the reason that the vapor pressure of ZnO is smaller than that of CdO at this growth temperature. The similar behavior was observed in ZnMgO[20] and ZnCaO.[21]

Figure 2 shows the ordinary (a) and logarithmic (b) XRD pattern of samples 1–6 and substrate. It can be noticed that only pronounced ZnCdO (0002) and ZnCdO (0004) peaks are observable besides the substrate diffraction peak at 41.71°. It indicates that the films have high single-orientation of the c axis. With the Cd concentration increasing, the characteristic diffraction peak of $Zn_{1-x}Cd_xO$ thin films shifts to a lower angle. According to the Bragg formula, the change in Bragg's angle due to the increasing of c-axis length of ZnCdO thin films, which suggests the Zn^{2+} is substituted by Cd^{2+} in ZnO lattices, successfully. Theoretically, since the ion radius of Cd^{2+} (0.92 Å) is larger than that of Zn^{2+} (0.74 Å), it can

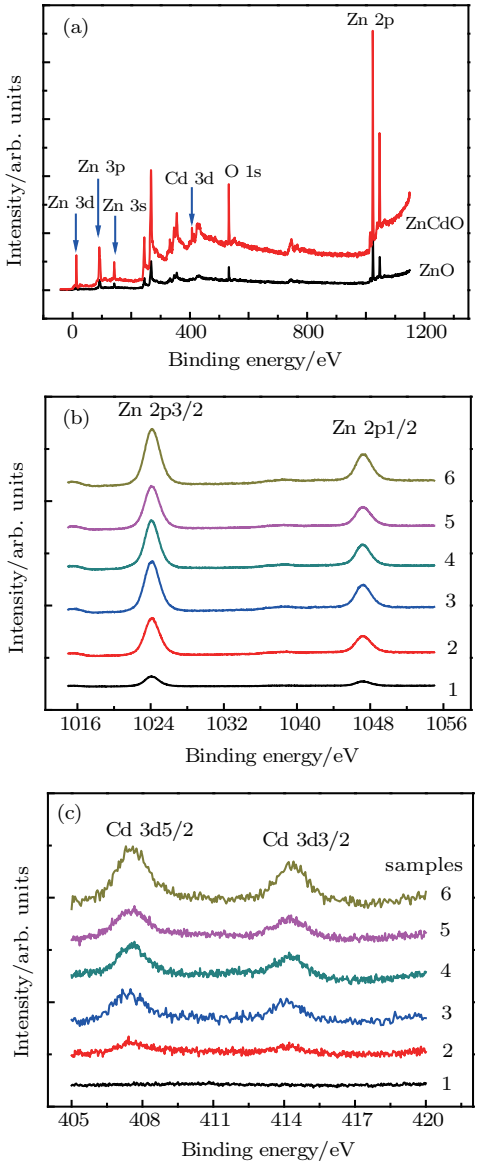


Fig. 1. (color online) XPS pattern of ZnCdO and ZnO thin films (a), Zn 2p (b), and Cd 3d (c) of samples 1–6.

Table 2. The composition, structural parameter, bandgap of ZnCdO thin films, and the band offset of ZnCdO/ZnO heterojunctions with different Cd concentrations.

Sample	x in targets/%	x in films/%	$2\theta/(^\circ)$	c axis/nm	E_g/eV	ΔE_V/eV	ΔE_C/eV
1	0	0	34.24	0.523	3.26	–	–
2	15	5.0	34.06	0.526	3.10	0.06±0.08	0.10±0.08
3	22.5	6.6	33.86	0.529	3.06	0.10±0.08	0.10±0.08
4	30	7.5	33.82	0.530	3.04	0.12±0.08	0.10±0.08
5	40	8.2	33.75	0.531	3.02	0.13±0.08	0.11±0.08
6	50	10.0	33.70	0.532	2.98	0.17±0.08	0.11±0.08

be concluded that the substitution of Zn by Cd atom induces the lattice volume expansion. Table 2 exhibits the values of ZnCdO (0002) characteristic diffraction peaks and the lattice constants of $Zn_{1-x}Cd_xO$ thin films, which are calculated by the Bragg diffraction formula $n\lambda = 2d\sin\theta$. Besides, the full width at half maximum (FWHM) of $Zn_{1-x}Cd_xO$ films has been obtained in Fig. 2(a). With the increasing of Cd concentration, the FWHM increases from 0.197° to 0.379°, which means the films crystal quality declines as the dopant content Cd increases.

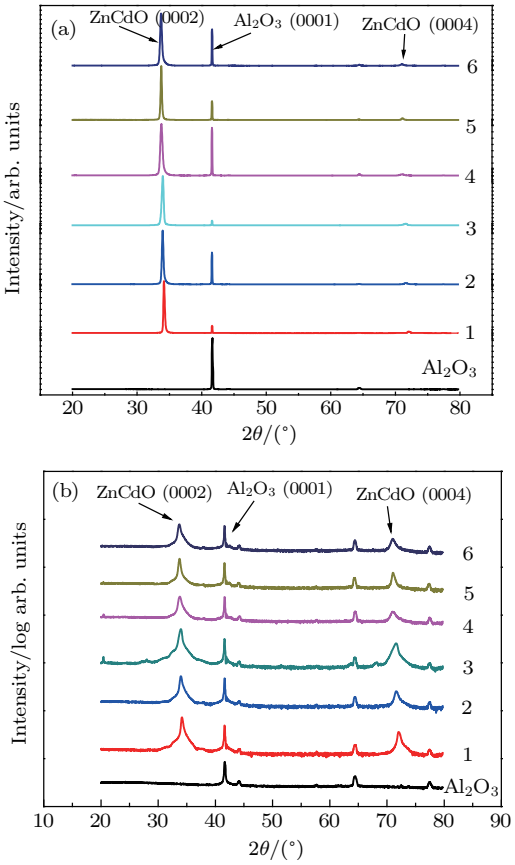


Fig. 2. (color online) The ordinary (a) and logarithmic (b) XRD pattern of $Zn_{1-x}Cd_xO$ films and substrate.

Using the UV-vis transmittance (T) and reflectance (R), combining with the optical absorption coefficient approximation formula:[22]

$$\alpha = \frac{1}{d} \times \ln\left(\frac{1-R}{T}\right), \tag{1}$$

the UV-vis absorption coefficient α of $Zn_{1-x}Cd_xO$ thin films is obtained, as shown in Fig. 3. The optical bandgap E_g of the $Zn_{1-x}Cd_xO$ thin films is gained by the Tauc relationship:[23]

$$(\alpha h\nu)^2 = A(h\nu - E_g), \tag{2}$$

where α, A, $h\nu$, E_g are the absorption coefficient, bandgap constant, photoenergy, and optical bandgap, respectively. The results are shown in Fig. 4 and the parameters are listed in Table 2. In addition, the $(\alpha h\nu)^2$–$h\nu$ curve of samples 1∼6 shift toward lower energy with the increasing of the Cd concentration mainly due to the hybrid effect of Cd 5s and Zn 4s, and the enhancement of the p–d repulsion effect of Zn 3d and Cd 4d with O 2p,[9,19] which will be explored in more detail in the following discussion. The bandgap of $Zn_{1-x}Cd_xO$ decreases with the increasing of Cd concentration, and the absorption threshold decreases too. The shift indicates that Cd atoms have been incorporated in the films.[24] It is necessary to notice that the bandgap of $Zn_{1-x}Cd_xO$ films would decrease further with the increasing of Cd concentration by adjusting other preparation conditions, such as pulse frequency, oxygen pressure, laser power density, and growth temperature.[17,25,26]

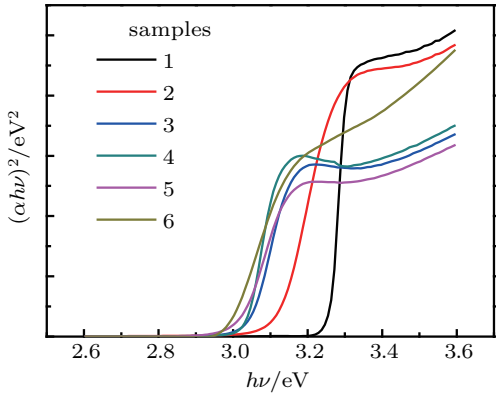


Fig. 3. (color online) The $(\alpha h\nu)^2$–$h\nu$ curve of $Zn_{1-x}Cd_xO$ films with different Cd concentrations.

The experimental results of samples 1–6 are fitted by the following conventional formula

$$E_g = xE_g^{CdO} + (1-x)E_g^{ZnO} - bx(1-x), \tag{3}$$

where E_g^{ZnO} and E_g^{CdO} represent the bandgap values of ZnO and CdO at room temperature, respectively. b is the bowing parameter, which depends on the difference electronegativities of CdO and ZnO. In this case, the bowing parameter is 2.1, which is lower than the previous result of 5.93,[8] and

greater than the recent reported value of 0.95.[27] The discrepancy may be ascribed to: (i) the neglection of the excitonic contribution, which would lead to E_g values decreasing about 100 meV,[27] (ii) the density of localization states, which changes with the Cd doping and then affects the value of the absorption edge.[10]

In our experiment, the different bandgap of ZnO and $Zn_{1-x}Cd_xO$ is sufficient to provide bandgap discontinuity in the heterostructure. The ΔE_V of $Zn_{1-x}Cd_xO$/ZnO heterojunctions can be determined by the following equation[23]

$$\Delta E_V = (E_{Zn\ 2p} - E_{VBM})_{ZnO} - (E_{Zn\ 2p} - E_{VBM})_{ZnCdO} + \Delta E_{CL}, \quad (4)$$

where $(E_{Zn\ 2p} - E_V)_{ZnO}$, $(E_{Zn\ 2p} - E_V)_{ZnCdO}$ are the CLs reference to the valence band maximum (VBM) energy of ZnO and ZnCdO thin films surface, respectively. The FWHM of Zn 2p3/2 peak of $Zn_{0.9}Cd_{0.1}O$/ZnO has no obvious difference with that of Zn 2p3/2 in the ZnO and $Zn_{0.9}Cd_{0.1}O$ films, as shown in Fig. 5(c). Therefore, we have[5]

$$\Delta E_{CL} = (E_{Zn\ 2p} - E_{Zn\ 2p})_{ZnCdO/ZnO} = 0. \quad (5)$$

The XPS results of $Zn_{0.9}Cd_{0.1}O$/ZnO heterojunction are shown in Fig. 5.

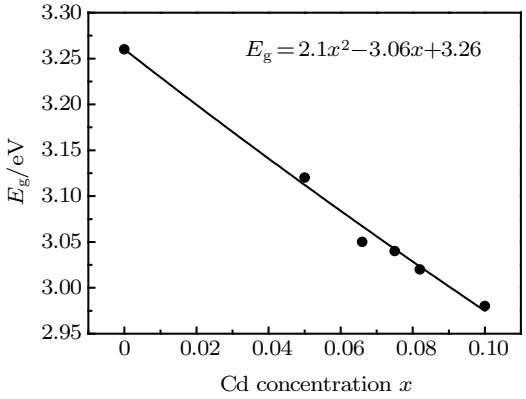


Fig. 4. The variation in bandgap energy (E_g) as a function of Cd concentration (x) of $Zn_{1-x}Cd_xO$ films.

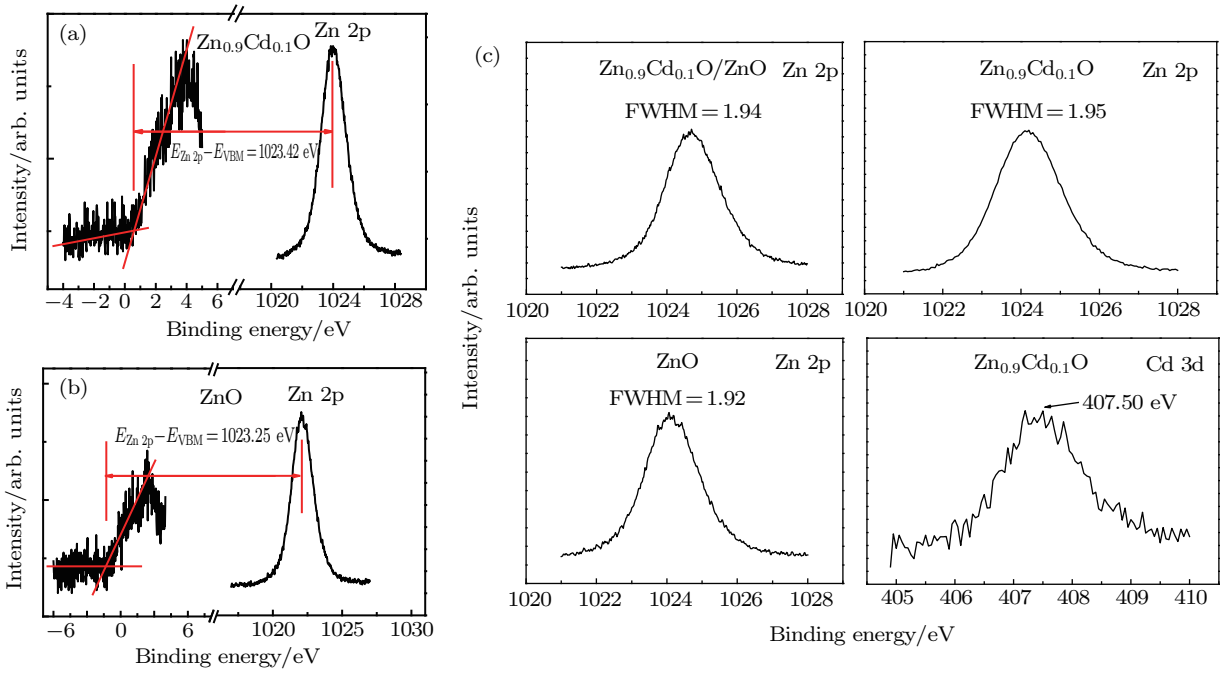


Fig. 5. (color online) XPS core levels (CLs) of Zn 2p3/2 and the valence band maximum of $Zn_{0.9}Cd_{0.1}O$ (a) and ZnO (b) thin films; XPS core levels (CLs) of Zn 2p3/2 of $Zn_{0.9}Cd_{0.1}O$/ZnO, $Zn_{0.9}Cd_{0.1}O$, ZnO, and Cd 3d of $Zn_{0.9}Cd_{0.1}O$ (c).

As shown in Figs. 5(a) and 5(b), the values of VBM are obtained by linear extrapolation of the leading edge to the extended base line. This method has been used to determine the VBM of the heterojunction, widely.[5,18,28] As a result, the energy difference of Zn2p CLs to VBM is determined to be 1023.42±0.04 eV in $Zn_{0.9}Cd_{0.1}O$ film. Similarly, the energy difference of Zn2p CLs to VBM is determined to be 1023.25±0.04 eV in ZnO film. ΔE_V is 0.17±0.08 eV by substituting the experimental values into Eq. (4), which is larger than $In_{0.2}Ga_{0.8}N$/GaN(0.06 eV).[29] The ΔE_C can be obtained by the formula $\Delta E_C = \Delta E_g - \Delta E_V$. ΔE_g (0.28 eV) is determined by the bandgap of ZnO (3.26 eV) and $Zn_{0.9}Cd_{0.1}O$ (2.98 eV) at room temperature, then the value of ΔE_C (0.11±0.08 eV) is obtained, which is lower than ΔE_V, suggesting that the electron is the dominant transport carrier. All the band offsets of samples 2–6 have been obtained by using the same method. The results have been shown in Table 2. It is found that the value of $\Delta E_C/\Delta E_V$ is close to 2:1 in the $Zn_{0.95}Cd_{0.05}O$/ZnO heterojunction, which was obtained by Chen.[18] Besides, the ΔE_V and ΔE_C increase with the increasing of Cd concentration, owing to the conduction band belonging to Zn 4s and Cd 5s, and the valence band derives from O 2p. Due to

the hybrid effect of Cd 5s and Zn 4s, with the increasing of Cd concentration, the conduction band offset declines continually until closing to Cd 5s. On the other hand, owing to the p–d repulsion effect of Zn 3d and Cd 4d with O 2p gradually enhanced,[9,19,30] the anion p electron orbit will be pushed to a higher energy state. The band diagram of the $Zn_{0.9}Cd_{0.1}O$/ZnO heterostructure interface is shown in Fig. 6. Both of the CBM (conduction band minimum) and VBM are on the ZnCdO side, indicating that the heterojunction belongs to the type-I alignment.

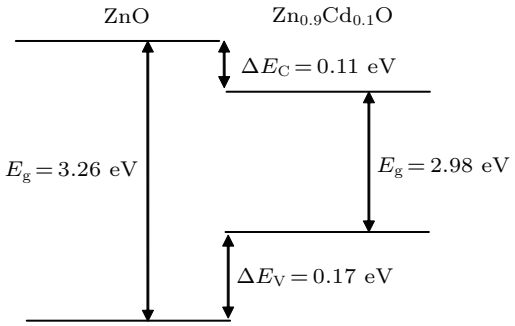


Fig. 6. Energy band diagram of the $Zn_{0.9}Cd_{0.1}O$/ZnO heterostructure interface.

4. Conclusion

In summary, $Zn_{1-x}Cd_xO$ thin films and $Zn_{1-x}Cd_xO$/ZnO heterojunctions have been fabricated on sapphire substrates by PLD. The structural and optical properties of the films with different Cd concentrations have been investigated. The XRD pattern shows that ZnCdO film grows along the *c* axis without any Cd-related phase. The UV-vis absorption coefficient α has been obtained by transmittance (T) and reflectance (R). The accurate relationships between the optical bandgap of $Zn_{1-x}Cd_xO$ films and the Cd concentration have been analyzed. Finally, the band offset of $Zn_{1-x}Cd_xO$/ZnO heterojunctions has been determined by XPS, which indicates that the band diagram belongs to type-I alignment. The band offset can be precisely adjusted through regulating the Cd concentration, and the ΔE_V of 0.17 eV is relatively good for application in p–n junctions and quantum well-related devices.

References

[1] Tsukazaki A, Ohtomo A, Onuma T, Ohtani M, Makino T, Sumiya M, Ohtani K, Chichibu S F, Fuke S, Segawa Y, Ohno H, Koinuma H and Kawasaki M 2005 *Nat. Mater.* **4** 42
[2] Wei Z P, Lu Y M, Shen D Z, Zhang Z Z, Yao B, Li B H, Zhang J Y, Zhao D X, Fan X W and Tang Z K 2007 *Appl. Phys. Lett.* **90** 042113
[3] Yang C, Li X M, Gu Y F, Yu W D, Gao X D and Zhang Y W 2008 *Appl. Phys. Lett.* **93** 112114
[4] Hu Z F, Wu H H, Lv Y W and Zhang X Q 2015 *Chin. Phys. B* **24** 107302
[5] Su S C, Lu Y M, Zhang Z Z, Shan C X, Li B H, Shen D Z, Yao B, Zhang J Y, Zhao D X and Fan X W 2008 *Appl. Phys. Lett.* **93** 082108
[6] Misra K P, Shukla R K and Srivastava A 2009 *Appl. Phys. Lett.* **95** 031901
[7] Liu Y R, Zhao G W, Lai T and Yao R H 2016 *Chin. Phys. B* **25** 088503
[8] Makino T, Segawa Y, Kawasaki M, Ohtomo A, Shiroki R, Tamura K, Yasuda T and Koinuma H 2001 *Appl. Phys. Lett.* **78** 1237
[9] Tang X, Lü H F, Ma C Y, Zhao J J and Zhang Q Y 2008 *Acta Phys. Sin.* **57** 1066 (in Chinese)
[10] Kang H. S, Kim J. W, Kim J. H, Lee S Y, Li Y, Lee J S, Lee J K, Nastasi M A, Crooker S A and Jia Q X 2006 *J. Appl. Phys.* **99** 066113
[11] Li G, Zhu X B, Tang X W, Song W H, Yang Z R, Dai J M, Sun Y P, Pan X and Dai S Y 2011 *J. Alloys Compd.* **509** 4816
[12] Yang W F, Liu B, Chen R, Wong L M, Wang S J and Sun H D 2010 *Appl. Phys. Lett.* **97** 061911
[13] Yamamoto K, Tsuboi T, Ohashi T, Tawara T, Gotoh H, Nakamura A and Temmyo J 2010 *J. Cryst. Growth* **312** 1703
[14] Ma D W, Ye Z Z, Lu H M, Huanga J Y, Zhao B H, Zhu L P, Zhang H J and He P M 2004 *Thin Solid Films* **461** 250
[15] Hu W S, Liu Z G, Sun J, Zhu S N, Xu Q Q, Feng D and Ji Z M 1997 *J. Phys. Chem. Solids* **58** 853
[16] Sadofev S, Blumstengel S, Cui J, Puls J, Rogaschewski S, Schafer P and Henneberger F 2006 *Appl. Phys. Lett.* **89** 201907
[17] Lei H W, Yan D W, Zhang H, Wang X M, Yao G, Wu W D and Zhao Y 2014 *Chin. Phys. B.* **23** 126104
[18] Chen J J, Ren F, Li Y J, Norton D P, Pearton S J, Osinsky A, Dong J W, Chow P P and Weaver J F 2005 *Appl. Phys. Lett.* **87** 192106
[19] Luo M H, Li M K, Zhu J K, Huang Z B, Yang H and He Y B 2016 *Acta Phys. Sin.* **65** 157303 (in Chinese)
[20] Ohtomo A, Kawasaki M, Koida T, Masubuchi K, Koinuma H, Sakurai Y, Yoshada Y, Yasuda T and Segewa Y 1998 *Appl. Phys. Lett.* **72** 2466
[21] Cao L, Jiang J and Zhu L P 2013 *Mater. Lett.* **100** 201
[22] Xin Y C, Zhou H J, Ni X J, Pan Y, Zhang X L, Zheng J Y, Bao S H and Jin P 2015 *RSC Adv.* **5** 57757
[23] Waldro J R, Grant R W, Kowalczyk S P and Kraut E A 1985 *J. Vac. Sci. Technol. A* **3** 835
[24] Jang D Y, Shen D Z, Liu K W, Shan C X, Zhao Y M, Yang T, Yao B, Lu Y M and Zhang J Y 2008 *Semicond. Sci. Technol.* **23** 035002
[25] Ma X Y, Chen P L, Zhang R J and Yang D R 2011 *J. Alloys Compd.* **509** 6599
[26] Ishihara J, Nakamura A, Shigemori S, Aoki T and Temmyo J 2006 *Appl. Phys. Lett.* **89** 091914
[27] Wang X J, Buyanova I A, Chen W M, Izadifard M, Rawal S, Norton D P, Pearton S J, Osinsky A, Dong J W and Dabiran A 2006 *Appl. Phys. Lett.* **89** 151909
[28] Li Y F, Yao B, Lu Y M, Li B H, Gai Y Q, Cong C X, Zhang Z Z, Zhao D X, Zhang J Y, Shen D Z and Fan X W 2008 *Appl. Phys. Lett.* **92** 192116
[29] Chris G, Van D W and Neugebauer J 1997 *Appl. Phys. Lett.* **70** 2577
[30] Yu X X, Zhou Y, Liu J, Jin H B, Fang X Y and Cao M S 2015 *Chin. Phys. B* **24** 127307